Time Dependence of Loudspeaker Power Output in Small Rooms*

GLYN ADAMS

School of Electrical Engineering, University of Sydney, NSW 2006, Australia

Some new calculations are described which are based on the method of image sources for determining the power output of a sound source operating within the boundaries of a listening room. Although it is well known that the power output of the source is influenced by the near boundaries, the dependence of power output on the nature of the room resonances has been largely overlooked. The analysis presented shows that the near boundary effects are defined by the early part of a general solution evaluated as a function of time after the signal is applied. The solution for time increasing toward steady state shows the progressive influence of the room resonances as they build up.

0 INTRODUCTION

Loudspeaker engineers have been aware for some time that the acoustic power output of a loudspeaker sound source is modified with respect to the free-field condition when the source is operated within the listening room. The best known studies in the audio field are those of Allison [1], [2], in which the influence of the three room boundaries nearest the source are determined. Allison's calculations of the source power were based chiefly on the earlier theoretical studies of Waterhouse [3]. A more recent paper by Ballagh [4] studies the optimization of source-to-boundary distances, but once again attention is confined to the influence of only the three nearest room boundaries.

The assumption that the influence of the remaining three room boundaries (that is, those farthest from the sound source) can be neglected has been based on a consideration of the distance of these boundaries from the source in terms of the wavelength of sound in air. The extension of the results for the near boundaries to those of the far boundaries in this way is unfortunately erroneous because it fails to take any account of the fact that the six room boundaries form a resonant enclosure. The resonances of this enclosure do in fact significantly influence the power output of the sound source—and particularly so at low frequencies [5]–[9].

In this paper a general solution for the power output of the sound source is developed by extending the method of images used by Waterhouse [3]. Because of the physical nature of this image model, it is easy to see that the power output of the source must actually be a function of time during the interval between the application of the excitation signal and the establishment of a steady-state sound field.

1 ANALYSIS

Consider first of all the case where the sound source is placed a distance x away from a single solid boundary of infinite extent, as shown in Fig. 1. If the boundary is a perfect reflector, then as far as an observer at some arbitrary point O is concerned, the reflection appears to be radiating from an image of the sound source positioned a distance x behind the boundary, as shown. For the purposes of calculation of the sound field, the boundary can thus be removed, and the problem treated as if the two sources were both radiating into free space.

Let the loudspeaker sound source, hereafter referred to as the main source—to distinguish it from the image sources—be represented by a small spherical sound source of radius a. If the surface of this simple source is made to pulsate sinusoidally with a normal velocity u, then the acoustic power radiated by the source is given by [10]–[12]

$$W = U_{\text{rms}}^2 R \tag{1}$$

* Presented at the 84th Convention of the Audio Engineering Society, Paris, France, 1988 March 1–4.

where $U = 4\pi a^2 u$ is the volume velocity, and R is the acoustic radiation resistance. The latter is the real component of the complex radiation impedance Z, where

$$Z = \frac{p}{U} = R + jX . \quad (2)$$

Here p is the pressure on the surface of the source, and $j = \sqrt{-1}$.

When the main source is radiating by itself into free space, the pressure p is due only to that generated by the main source. The radiation impedance under this condition is [10]–[12]

$$Z_f = R_f + jX_f = \frac{\rho ck^2}{4\pi} + j\frac{\rho ck}{4\pi a} \quad (3)$$

where ρ is the density of air, c is the velocity of sound in air, k is the wave number, $= 2\pi f/c$, and f is the frequency. Eq. (3) is valid provided that $k^2a^2 << 1$.

The "self"-pressure of the main source can thus be written from Eqs. (2) and (3) as

$$p_{self} = U\left[\frac{\rho ck^2}{4\pi} + j\frac{\rho ck}{4\pi a}\right] . \quad (4)$$

The image source introduced to represent the boundary reflection also makes a contribution to the sound pressure at the surface of the main source. Because p is modified in this way, it is clear from Eqs. (1) and (2) that R and hence the power output W are modified by the reflection. The sound pressure at a distance r from the image source radiating by itself into free space is given by [10]–[12]

$$p_{image} = j\frac{Uf\rho\, e^{-jk(r-a)}}{2r} \quad (5)$$

where strength U and radius a are the same as that of the main source—as would be the case when modeling a perfect reflection.

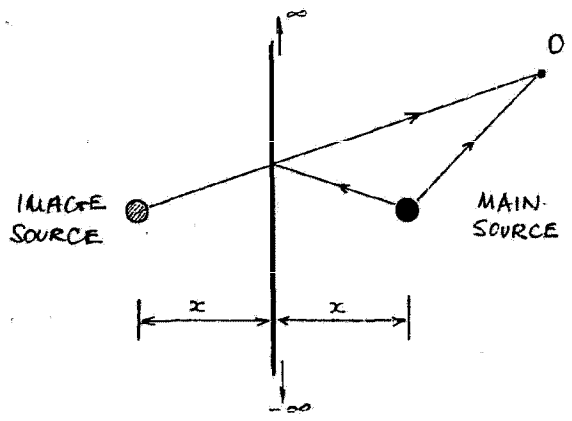

Fig. 1. Image model for single reflection.

If a is small such that $a << r$, then the pressure contribution at the surface of the main source due to the image is

$$p_{image} = j\frac{Uf\rho e^{-jk2x}}{4x} \quad (6)$$

which can be written

$$p_{image} = \frac{\rho ck}{8\pi x} U(\sin 2kx + j\cos 2kx) . \quad (7)$$

Taking both sources into account, the pressure at the surface of the main source is $p_{self} + p_{image}$, and thus the radiation impedance of the main source is given by

$$Z = \frac{p_{self} + p_{image}}{U} . \quad (8)$$

The real component of Z gives the radiation resistance, that is,

$$R = \frac{\rho ck^2}{4\pi} + \frac{\rho ck}{8\pi x}\sin 2kx \quad (9)$$

$$= \frac{\rho ck^2}{4\pi}\left(1 + \frac{\sin 2kx}{2kx}\right) \quad (10)$$

$$= R_f\left(1 + \frac{\sin 2kx}{2kx}\right) . \quad (11)$$

If the value of the source strength U is unaffected by the increased acoustical loading due to p_{image}, then the power output of the main source is given by

$$\frac{W}{W_f} = \frac{R}{R_f} = 1 + \frac{\sin 2kx}{2kx} \quad (12)$$

where W_f is the power output of the main source in free space.

For a typical moving-coil direct-radiator-type loudspeaker system, the diaphragm velocity u is hardly influenced at all by the environment in which the loudspeaker system is placed [7]. Eq. (12) thus closely approximates the power output modification we can expect for a loudspeaker system of this type operating near a single solid boundary.

2 IMAGE MODEL OF RECTANGULAR ROOM

When the sound source is placed near three mutually perpendicular boundaries, the reflections can be represented by seven image sources as illustrated in Fig. 2. The power output of the main source of such an arrangement can be found by following the same formulation developed in Sec. 1, but noting that the pressure p in the numerator of Eq. (8) is now the sum of

the self-pressure and the pressure contributions of seven images. Thus we can write

$$\frac{W}{W_f} = 1 + \sum_{i=1}^{7} \frac{\sin kd_i}{kd_i} \tag{13}$$

where d_i ($i = 1, \ldots, 7$) are the distances from the main source to each image source. If the main source is placed at distances x, y, z normal to the three boundaries, then Eq. (13) becomes directly equivalent to the expressions used by Waterhouse and Allison.

By introducing the three boundaries farthest from the source we complete the enclosure of the source within a rectangular room. The first reflections from the near boundaries and the direct sound wave from the main source now undergo successive reflections as the sound waves bounce to and fro between the six room boundaries. As before, these reflections can be represented by image sources, as illustrated in Fig. 3.

The positions of the new images can be found by tracing out the paths of each reflection in the normal way. However, a regular pattern of images soon emerges such that the geometry for images of higher order is easily found with some simple vector algebra. In general, the "cluster" of eight sources formed within the corner of the boundaries nearest the main source generates an infinite number of images of itself extending in all directions with positions defined by a three-dimensional rectangular grid. The spacing of the grid lines is equal to $2l_x$, $2l_y$, $2l_z$, where l_x, l_y, l_z are the room dimensions.

Computation of the power output of the main source operating within the room simply involves the extension of the summation defined in Eq. (13) to include all of the additional image sources. Thus we can write

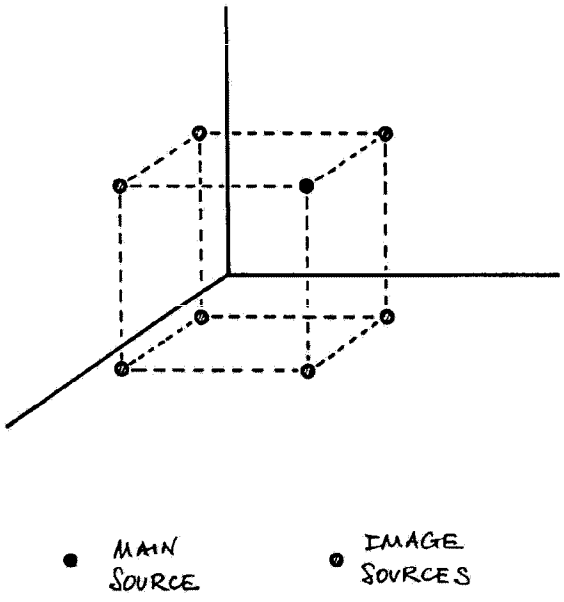

Fig. 2. Image cluster formed at corner of three boundaries.

$$\frac{W}{W_f} = 1 + \sum_{i=1}^{\infty} \frac{\sin kd_i}{kd_i} . \tag{14}$$

This equation and the three-dimensional arrangement of extending images demonstrate the importance of including the influence of the far boundaries. Although the images are increasingly distant from the main source, thus reducing their contribution to the sum, the *number* of images within a certain range rises with increasing distance. This compensating effect means that the distant images are equally important, and in fact Eq. (14) does not converge within a finite number of images.

An intuitive study of the image model also enables us to see why the power output of the main source will be dependent on room resonances. The regular grid of image sources will clearly give rise to some pressure contributions arriving at the main source which, at particular frequencies, will all be in phase with each other. The power output will thus be increased to a greater extent at these frequencies than at other frequencies. For example, consider the contributions from the many sources spaced at regular intervals of $2l_x$. When this spacing is equal to an integral number of wavelengths, the contributions will arrive in phase. This condition is of course equivalent to $f_n = nc/2l_x$, where $n = 1, 2, 3, \ldots$, and f_n are the frequencies of the axial resonance modes in the x direction.

Lack of convergence of Eq. (14) is not very helpful from a computational point of view. However, in practice, real room boundaries are not perfect reflectors, and thus the strength of an image source is always less than that of the main source. If the boundaries have a frequency-independent reflection coefficient β, then the strength of the image source used in Eq. (6) is changed to βU. Eq. (12) then becomes

$$\frac{W}{W_f} = 1 + \beta \frac{\sin 2kx}{2kx} . \tag{15}$$

In forming higher order images, that is, when an image undergoes successive reflections, the strengths steadily reduce in a manner $\beta^2 U, \beta^3 U, \ldots$. The general summation can thus be written

$$\frac{W}{W_f} = 1 + \sum_{i=1}^{m} \beta^{nr(i)} \frac{\sin kd_i}{kd_i} \tag{16}$$

where the sum is now over a finite number of images m, and $nr(i)$ is the number of reflections which the ith image has been through. The value of m is chosen so that any further contributions to the sum have a negligible effect on the total. Smaller values of β enable convergence to be achieved with smaller values of m.

3 TIME DEPENDENCE

If the main source is switched on at time $t = 0$, then all of the image sources are also considered to have been switched on at this time. It will clearly take some

time before the sound-pressure contributions of all of the m images reach the main source such that a steady-state condition is reached. If we denote this time by t_{ss}, then from the geometry of the image model we can see that the pressure at the surface of the main source, and hence its power output, will be changing during the time period $0 \rightarrow t_{ss}$ as the contributions from the various images arrive one after the other. The power output at any time during this period is given by

$$\frac{W(t)}{W_f} = 1 + \sum_{i=1}^{N(t)} \beta^{nr(i)} \frac{\sin kd_i}{kd_i} \qquad (17)$$

where $i = 1, \ldots, N(t)$ includes only those images that are contained within a sphere centered on the main source and whose radius is equal to ct. When this radius extends to ct_{ss}, then $N(t) = m$.

Fig. 4 illustrates the process of including more and more images as time proceeds. For small values of t such that only the main source and the first seven images are contained within the sphere (that is, $N = 7$, $t = 0+$), then the power output follows the well-known solution for the near-boundary effects. It would thus be sensible to consider that particular solution as applying to the "early sound wave" comprising the direct sound from the source and the first reflections from the near boundaries. As time goes on, this "early" solution is progresively modified, and as shown in the next section, the power output curve eventually displays a number of resonance peaks and dips.

This method of predicting the time behavior of the sound field within the room follows from a very similar approach adopted by Eyring [13] in his calculations of the reverberation time of the room.

4 SOME EXAMPLES

The summation of Eq. (17) was solved as a function of frequency for several different times t between 0 and t_{ss}. The algorithms for determining the distance d_i and the number of reflections $nr(i)$ relating to each image were developed along similar lines to those given by Allen and Berkely [14].

A room of dimensions $l_x = 6$ m, $l_y = 5$ m, and $l_z =$

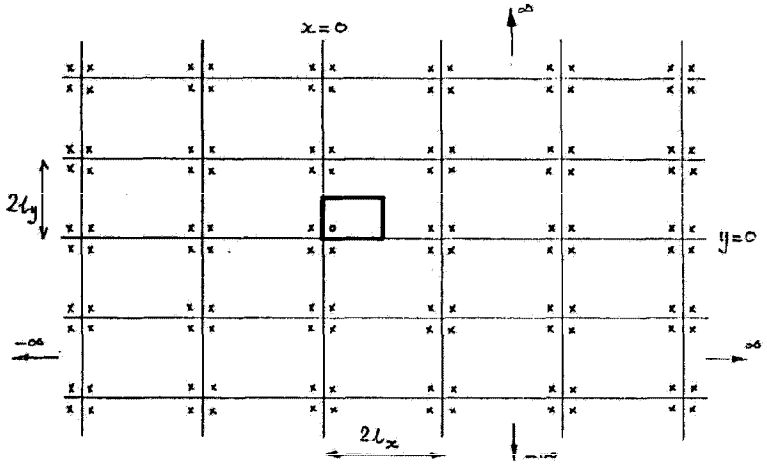

Fig. 3. Image model for source operating in rectangular room. The rectangular lattice of image sources also extends above and below the room with a spacing of $2l_z$.

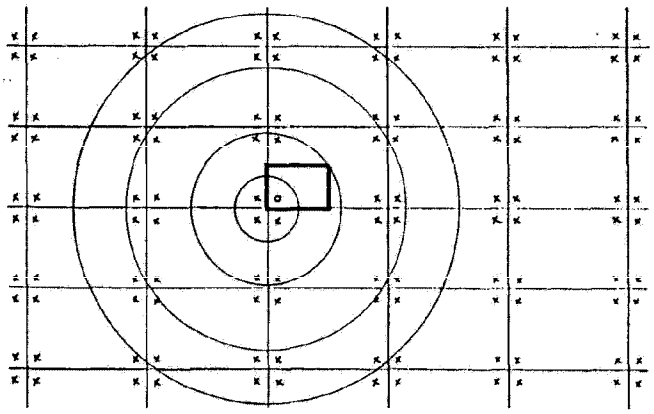

Fig. 4. Concept of an expanding sphere, which includes more and more image sources corresponding to time increasing after source excitation.

3.5 m was chosen, having walls with a reflection coefficient $\beta = 0.9$. The main sound source was placed at $x = y = z = 1$ m. A guide to the expected value of t_{ss} was obtained by computing the reverberation time of the room using Eyring's formula [11]. This room has a reverberation time of about 1 s, which is not an untypical value for a real domestic listening room at low frequencies. In practice the summation converges in a shorter time than the reverberation time—as might be expected because a "60-dB down" contribution will not have much effect on the total. A value of t_{ss} of about half the reverberation time will probably be adequate.

Fig. 5 shows the value of W/W_f computed for t equal 0+ such that only the first seven images are taken into account. This is equivalent to the well-known three-boundary solution. The power output of the source is mostly modified in the low-frequency range, and thus further examples will concentrate on the range up to 200 Hz.

Figs. 6–11 show the value of W/W_f computed for t equal to 0+, 50, 100, 150, 300, and 500 ms, respectively. Fig. 11 also shows the "early"curve for comparison. The similarity of the figures for $t = 300$ and $t = 500$ ms suggests that the sum has converged by this time. As time increases from 0, a steady modification of the power curve is evident, with fairly wide-band variations being introduced initially, but changing at later times to a more narrow-band form with peaks developing in the vicinity of the room resonances. In general, the power output is increased above the early value at these resonance peaks, but is sometimes reduced below the early value at intermediate frequencies.

The early and late power curves shown in Fig. 11 demonstrate an interesting similarity in overall shape. This suggests that the trend of the early power curve can be thought of as remaining during the buildup period (the other figures support this), the effects of room resonance and antiresonance then being progressively added to this trend.

Finally, Fig. 12 shows the $t = 500$ ms power curve computed for a reflection coefficient $\beta = 0.8$. This corresponds to a reverberation time of about 0.5 s—a level that is typically achieved at low frequencies in specially constructed monitoring rooms and studios. Because the room resonances are now better damped, the power variation with frequency is reduced compared to that of the more lively room.

5 CONCLUSIONS

This paper has examined a more complete treatment of the change in power output that we can expect when a loudspeaker is placed within a rectangular room. Earlier studies have mostly concentrated on the effects of the three nearest boundaries to the source, but such a solution is not really complete. By developing a solution which incorporates the influence of all six room boundaries, it has been shown that:

1) The power output at low frequencies is strongly influenced by resonances of the room, variations of the order of 10:1 being typical.

2) When the sound source is first switched on, the power output changes as a function of time up until a steady-state sound field is established. This time period is typically about half the reverberation time of the room.

3) The power output curve at a time shortly after the source is switched on has the same form as the simplified solution which considers only the three nearest boundaries. This particular solution could thus be considered

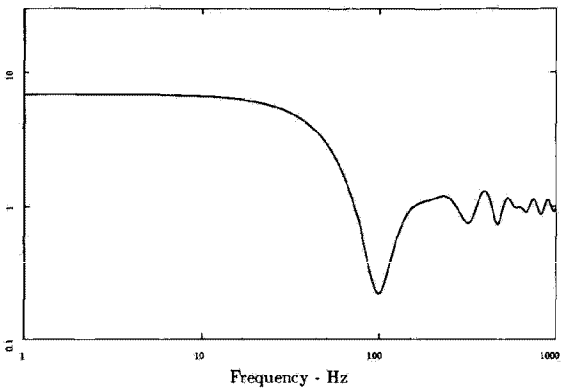

Fig. 5. Power output curve for "early" time period; $t = 0+$.

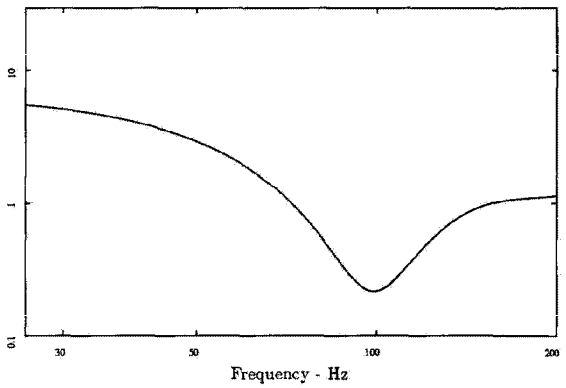

Fig. 6. As Fig. 5, but up to 200 Hz only; $t = 0+$

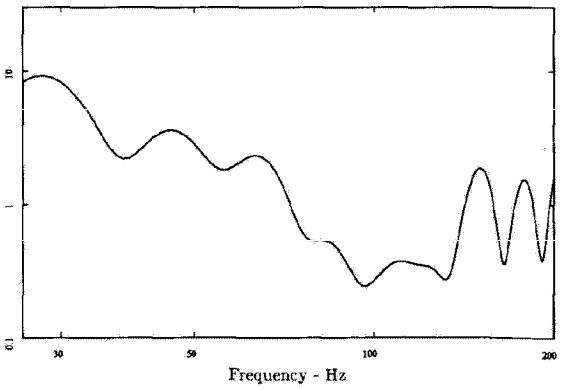

Fig. 7. Power output curve at $t = 50$ ms.

as applying to the "early sound wave," comprising the direct sound wave from the main source and the first reflections from the nearest boundaries.

4) The power curve for steady-state conditions retains a trend in shape which follows the curve for the early sound wave. This means that choices of the source displacements x, y, z based on obtaining a smooth curve from the simplified near-boundary solution may not in fact be far off the optimum.

6 REFERENCES

[1] R. F. Allison, "The Influence of Room Boundaries on Loudspeaker Power Output," *J. Audio Eng. Soc.*, vol. 22, pp. 314–320 (1974 June).

[2] R. F. Allison, "Influence of Listening Rooms on Loudspeaker Systems," *Audio*, vol. 63, pp. 36–40 (1979 Aug.).

[3] R. V. Waterhouse, "Output of a Sound Source in a Reverberation Chamber and Other Reflecting Environments," *J. Acoust. Soc. Am.*, vol. 30, pp. 4–13 (1958 Jan.).

[4] K. O. Ballagh, "Optimum Loudspeaker Placement Near Reflecting Planes," *J. Audio Eng. Soc.*, vol. 31, pp. 931–935 (1983 Dec.).

[5] T. Salava, "Performance Criteria for Loudspeakers in Rooms," presented at the 47th Convention of the Audio Engineering Society, *J. Audio Eng. Soc. (Abstracts)*, vol. 22, pp. 270, 272 (1974 May), preprint A3.

[6] T. Salava, "The Sound Field and the Acoustic Load of a Sound Source in a Rectangular Room," *Proc. IREE (Australia)*, vol. 37, pp. 60–62 (1976 Mar.).

[7] G. J. Adams, "Adaptive Control of Loudspeaker Frequency Response at Low Frequencies," presented at the 73rd Convention of the Audio Engineering Society, *J. Audio Eng. Soc. (Abstracts)*, vol. 31, p. 364

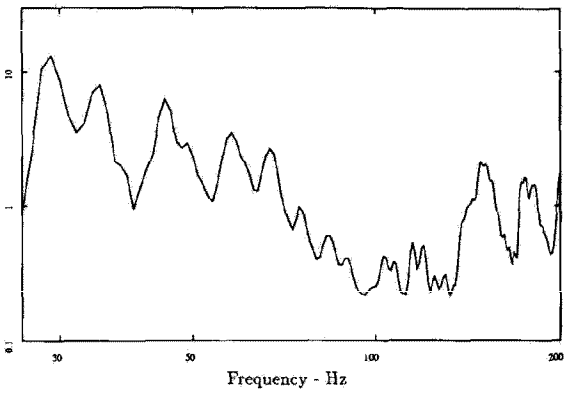

Fig. 10. Power output curve at t = 300 ms.

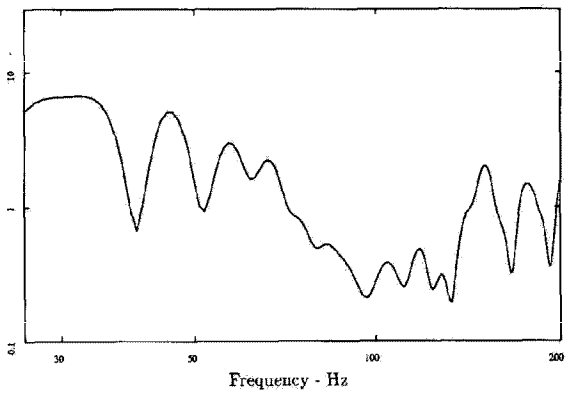

Fig. 8. Power output curve at t = 100 ms.

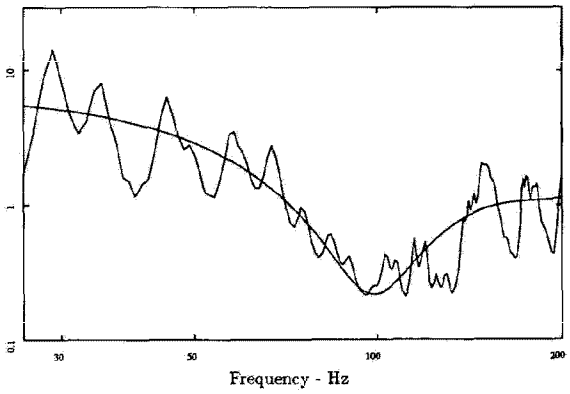

Fig. 11. Power output curve at t = 500 ms for β= 0.9.

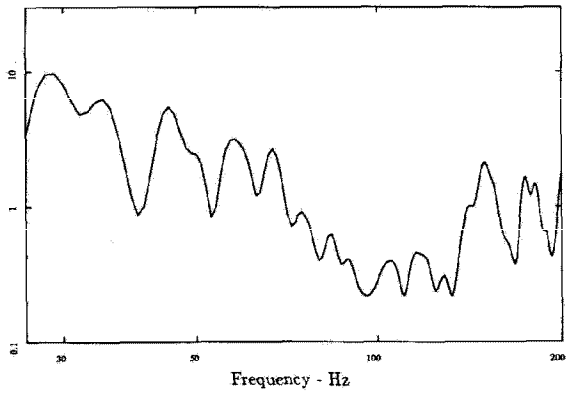

Fig. 9. Power output curve at t = 150 ms.

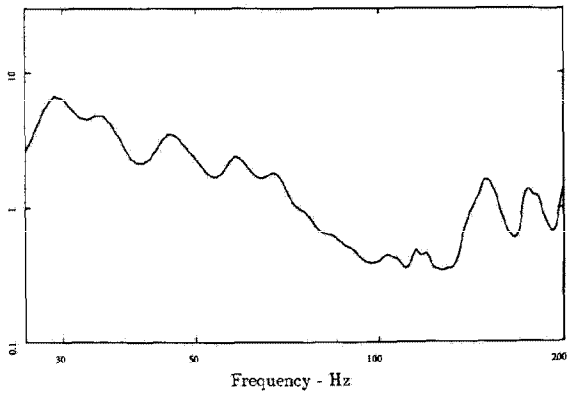

Fig. 12. Power output curve at t = 500 ms for β = 0.8.

(1983 May), preprint 1983.

[8] G. J. Adams, "Sound Power Output of Loudspeakers in Small Rooms," *Proc. Inst. Acoustics Autumn Conf.* (Windermere, UK, 1985).

[9] T. Salava, "Acoustic Load and Transfer Functions in Listening Rooms," presented at the 82nd Convention of the Audio Engineering Society, London, UK, 1987 March 10–13, preprint 2455.

[10] L. L. Beranek, *Acoustics* (McGraw-Hill, New York, 1954).

[11] L. E. Kinsler and A. R. Frey, *Fundamentals of Acoustics*, 2nd ed. (Wiley, New York, 1962).

[12] O. Jacobsen, "Some Aspects of the Self and Mutual Radiation Impedance Concept with Respect to Loudspeakers," *J. Audio Eng. Soc.*, vol. 24, pp. 82–92 (1976 Mar.).

[13] C. F. Eyring, "Reverberation Time in Dead Rooms," *J. Acoust. Soc. Am.*, vol. 1, pt. 1, pp. 217–241 (1930 Jan.).

[14] J. B. Allen and D. A. Berkley, "Image Method for Efficiently Simulating Small-Room Acoustics," *J. Acoust. Soc. Am.*, vol. 65, pp. 943–950 (1979 Apr.).

THE AUTHOR

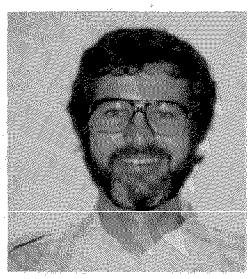

Glyn Adams was born in Henley-on-Thames, U.K, in 1954. He graduated with a First-Class Honors degree in electrical engineering from Southampton University in 1975 and continued his studies at Southampton under the supervision of Dr. Robert Yorke. He was awarded the degree of Ph.D. for work on the use of optimization and motional feedback techniques in loudspeaker system design in 1980.

Dr. Adams joined B&W Loudspeakers in 1978 as a senior project engineer, to work on the design and development of domestic high-fidelity loudspeaker systems. In 1983 he was appointed head of research and then concentrated on the measurement of loudspeaker diaphragm and enclosure vibration using laser interferometry techniques, and on the prediction of vibration and sound radiation using the finite element technique.

In 1986 Dr. Adams moved to Australia and took up a temporary position as an acoustic consultant with Robert Fitzell Acoustics. In 1987 February he was appointed lecturer in the School of Electrical Engineering, The University of Sydney, where he teaches electronics and signal processing. His current research interests are in the areas of digital signal processing, room acoustics simulation, and digital audio.

Dr. Adams is a member of the IEE and the AES.